12th Hungarian Conference on Theoretical and Applied Mechanics
HCTAM, 2015
August 25-27, 2015 Miskolc, Hungary

EXPLICIT MODEL OF CUMULATIVE SURFACE LOCATION ERROR FOR MILLING PROCESSES

Ádám Kiss[1] and Dániel Bachrathy[2]

[1,2]Department of Applied Mechanics, Budapest University of Technology and Economics
1111 Budapest, Műegyetem rkp. 5., Hungary
[1]kiss_a@mm.bme.hu, [2]bachrathy@mm.bme.hu

Abstract: *The aim of this study is to create mechanical model which is suitable to investigate the surface quality in milling processes, based on the Cumulative Surface Location Error (CSLE). This describes the series of the consecutive Surface Location Errors (SLE) in roughing operations. In the established model, the investigated CSLE depends on the previously resulted SLE by means of the variation of the radial immersion. The phenomenon of the system can be described as a discrete map. Flip- and fold type bifurcation and chaotic behaviour can be observed for CSLE. The stability boundaries of the flip- and fold type bifurcations are presented together with the traditional stability chart – which presents the chatter-free technological parameter domain.*

Keywords: *Machine tool vibration, surface quality, Surface Location Error, stability chart*

1. INTRODUCTION

In the industry for production and manufacturing, milling is a widely used method. However, high material removal rate often cannot be established in practice due to the instability of the cutting process. This machining process induces harmful vibrations which responsible for unacceptable surface quality. These vibrations are classified into two groups [1]. One of them is the self-excited vibration which comes from loss of stability of the periodic vibration due to the surface regeneration effect [2]. This effect can be modelled with delayed differential equations (DDE) [3]. The other type of vibration is the large amplitude forced vibration near to resonant spindle speeds [4].

The so-called stability chart [5] presents the chatter-free (stable) parameter domain which is usually illustrated along the parameters of the spindle speed and axial immersion, calculated by numerical methods [6, 7]. The stability boundary has pocket between the so-called stability lobes typically at the resonant spindle speed. The most productive parameter regions are located between the pockets of the lobes, where large amplitude vibration can occur due to the resonant spindle speed which leads substantial Surface Location Error (*SLE*) [8]. The stability chart is usually used at the roughing processes. Due to the fact, that *SLE* is relevant at finishing operations [9], its effect is usually neglected in the model of roughing operations, but despite this, it can has significant impact on the surface quality in case of consecutive immersions.

We introduce a new type of surface error calculation, which consider the effect of the series of *SLE*s during several consecutive immersion in roughing operations.

The oversize of a workpiece is removed with several consecutive immersions in roughing machining operations. At every immersion, the machined surface differs from the desired surface due to the Surface Location Error. The current offset error SLE_i modifies the next radial immersion and generates different cutting force, which leads to a modified subsequent SLE_{i+1}. During this process, the *SLE* can be accumulated and this phenomenon leads a new surface quality parameter denoted by the Cumulative Surface Location Error (*CSLE*) [10, 11]. The evaluation of the series of *SLE*s values and its stability problems are investigated in milling operations on a Single-Degree-of-Freedom (*SDoF*) mechanical model.

Computation of Surface Location Error

In the followings, the main steps of the *SLE* computation are summarised based on [12]. The quality of the machined surface property – specifically the so-called Surface Location Error (*SLE*) – is determined numerically in case of straight fluted tool. In the mechanical model, the workpiece is considered as a rigid body and the cutting tool is considered as *SDoF* as shown in Figure 1.

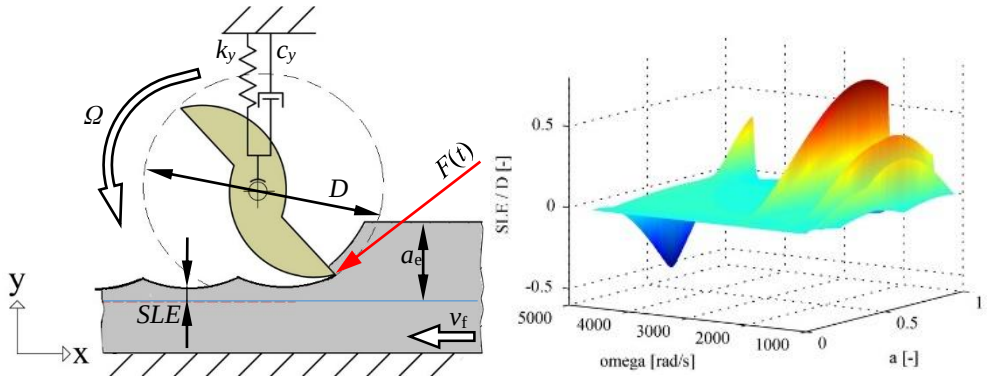

a) b)

Figure 1. a) Mechanical model of the cutting process; b) Surface Location Error in the function of spindle speed Ω and dimensionless radial immersion $a = a_e/D$, (Parameters: $w = 4$ mm; $z = 1$; $f_z = 0.1$ mm)

The cutting process is described with rotational main movement (spindle speed Ω) and feed movement v_f, which defined by $v_f = \frac{f_z \cdot N \cdot \Omega}{2 \cdot \pi}$, where f_z is the feed per tooth and N is the number of the teeth. The motion of the tool centre can be described as an inhomogeneous ordinary differential equation in the following forms

$$m_y \ddot{y}(t) + c_y \dot{y}(t) + k_y y(t) = F_y(t), \qquad (1)$$

where the dynamical parameters are defined in Table 1., y denotes the general coordinate of the tool centre and $F_y(t)$ is its exciting force. In this study, linear force model is considered [13] in which the force is linearly proportional to the chip width w and the chip thickness h. The chip thickness consist two parts, stationary and dynamic chip thickness [14]. The stationary one is resulted by the projection of the feed motion in the direction of the cutting edge $h_j(\varphi_j(t)) = f_z \sin(\varphi_j(t))$, where $\varphi_j(t)$ denotes the current angular position of the jth tooth's. The dynamic one corresponds to the surface regenerative effect of the machining process. Now only the periodic motion is analysed, hence only the stationer component of the chip thickness is used. The radial and tangential cutting force component is projected to the global coordinate system [15], therefore the exciting force along the y direction is given by

$$F_y(t) = \sum_{j=1}^{N} h_j\left(\varphi_j(t)\right)\, w\, g_j\left(\varphi_j(t)\right)\left(K_r \cos\left(\varphi_j(t)\right) - K_t \sin\left(\varphi_j(t)\right)\right), \qquad (2)$$

where $g_j(\varphi_j(t))$ is the screen function which indicates that the jth edge is in contact with the material or not. Its value is 1 when the angular position of the jth edge is between the entre φ_{ent} and exit angle φ_{exit}. These angles are the non-linear functions of the dimensionless radial immersion [16]:

$$\begin{aligned} &\text{Up-milling:} && \varphi_{ent} = 0, && \varphi_{exit} = \arccos(1 - 2a) \\ &\text{Down-milling:} && \varphi_{ent} = \arccos(2a - 1), && \varphi_{exit} = \pi \end{aligned} \qquad (3)$$

The periodic solution of the equation of motion (1) describes the vibration of the tool centre, whereby the path of the jth cutting edge $\mathbf{e}_j$ is defined. This solution is determined in frequency domain, based on the Fourier transformation. The surface contour is defined by the motion of the cutting edges and their vibrations leads to a constant offset error perpendicular to the desired surface. The maximum distance between the milled and desired surface is the so-called Surface Location Error (*SLE*). The *SLE* is defined by $SLE = \min(e_{y,j}(t) + D/2)$ in case of up-milling, $SLE = \max(e_{y,j}(t) - D/2)$ for down-milling, where $e_{y,j}$ is the y component of the path of the jth cutting edge.

The *SLE* depends on various cutting parameters. It is linearly proportional to the feed per tooth f_z and in case of straight-edged-tool it is linearly proportional to the axial immersion w due to the assumption that the cutting force is linearly proportional to these parameters. The spindle speed parameter Ω has a strong non-linear influence, since the natural frequencies of the system could be excited by the Fourier components of the cutting force which can lead to large resonant vibrations and large *SLE* values at certain so-called resonant spindle speeds. The *SLE* is a non-linear function of the radial immersion, too, as seen in Eq. 3. This influence has a key role of the following analysis, therefore, this function is denoted by $SLE = f_{SLE}(a)$, where dimensionless radial immersion $a = a_e/D$.

Traditionally, the axial immersion is denoted by a_p, and the radial immersion is denoted by a_e, however, in this study the w notation is used for axial immersion, hence they are equivalent in case straight-edged-tool. In the present study, all the computations performed for the parameters presented in Table 1., like modal parameters and the cutting coefficients corresponding to the material of the workpiece.

mass	damping	stiffness	material of the workpiece	Radial cutting coefficient	Tangential cutting coefficient
m_y = 0.02008 kg	$c_y = 1.15569 \frac{\text{Ns}}{\text{m}}$	$k_y = 413445 \frac{\text{N}}{\text{m}}$	AlMgSi0.5	$K_r = 2{,}369 \cdot 10^8 \frac{\text{N}}{\text{m}^2}$	$K_t = 6{,}44 \cdot 10^8 \frac{\text{N}}{\text{m}^2}$

Table 1. Modal parameters and cutting coefficients [17]

2. EVOLUTION OF THE CUMULATIVE SURFACE LOCATION ERROR

In the following sections, we consider the influence of the actual SLE_i on the dimensionless radial immersion of the subsequent cutting which leads to a modified error SLE_{i+1} (see in Figure 2.a). During the roughing process, one can set the desired dimensionless radial immersion a_0 which is modified by the actual SLE_i resulting the subsequent dimensionless radial immersion $a_{i+1} = a_0 + SLE_i/D$ and the subsequent error:

$$SLE_{i+1} = f_{SLE}\left(a_0 + \frac{SLE_i}{D}\right). \tag{4}$$

Equation (4) defines a discrete map– based on the dynamical milling model – which determines how one *SLE* develops into another *SLE* over a subsequent immersions. These series of the *SLE*s can converged to a fix point (see Figure 2.b), which is denoted by *CSLE*, and computed as a root of the following equation:

$$f_{SLE}\left(a_0 + \frac{CSLE}{D}\right) - CSLE = 0. \tag{5}$$

Solution methods

CSLE is the stationer solution of the map Eq. (4). This solution is obtained by two different methods. One of them is a numeric iteration of the map defined by (Eq. (4)) and the other is numerically calculated roots of the analytical function defined by Eq. (5), made by Multi-Dimensional Bisection Method [18].

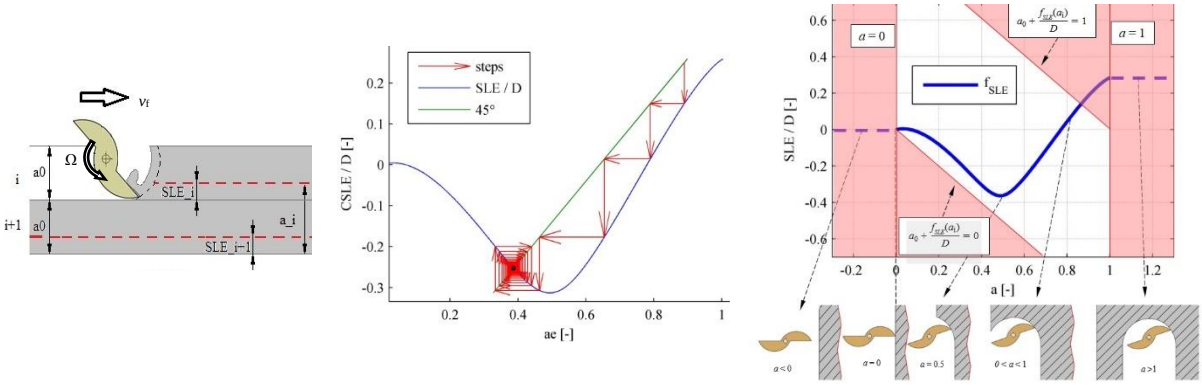

a) b) c)

Figure 2. a) Mechanical model of Cumulative Surface Location Error; b) Mapping of the fix point by means of numeric iteration; c) Validity range of f_{SLE}; mathematically extended model based on Eq. (6) and geometrical meanings (bottom figures); Red area: physically invalid range; Parameters: Ω = 4565 rad/s; w = 4 mm; z = 1 ; f_z = 0.1 mm

Validity range

Both the numerical methods could lead to numeric problems due to the fact that the f_{SLE} function has range of validity for the dimensionless radial immersion $a \in [0,1]$, which defines the vertical lines in Figure 2.c. In order to the mapping of the governing difference equation (4) remains in valid range, the subsequent dimensionless radial immersion a_{i+1} must be in the valid range ($a \in [0,1]$), too. For this purpose, the following equation has to be satisfied:

$$0 < a_0 + \frac{f_{SLE}(a_i)}{D} < 1. \tag{6}$$

This equation is represented by the slanting lines with slope of 45° in Figure 2.c. These lines represents the valid range of the calculation methods, denoted by white region in Figure 2.c. In case of very large tool vibration, the resultant *SLE* can be extremely large, therefore the dimensionless radial immersion value at a certain step of the iteration of the *CSLE* can fall outside from the range of validity and the calculation leads to error. In order to handle this, a mathematical approach is applied: the range of the validity of the f_{SLE} function is extended as follows

$$\begin{aligned} f_{SLE}(a > 1) &= f_{SLE}(1) \\ f_{SLE}(a < 0) &= f_{SLE}(0). \end{aligned} \tag{7}$$

This mathematical extension is valid in an engineering point of view, while, if a is bigger than 1, it represents a situation, when the tool is completely in the material and if a is smaller than 0, it represents a case, when the tool doesn't touch the surface and there is no machining at all, see the bottom part of Figure 2.c.

Using this theoretical extension of the *SLE* function, *CSLE* can be calculated in the entirely parameter space. This mathematically extended region can still lead to physically irrelevant solutions, however, these solutions can be filtered out easily.

With the extended validity range, CSLE is computed by both solution methods (MDBM and numeric iteration) for parameters presented in Table 1. As it is shown in Figure 3., the MDBM provides multiple solution of CSLE in the parameter range of $a \in [0.0525, 0.11]$. It is also validated by means of numeric iteration, where based on the various initial values of the iteration, the series of *SLE*s converges to different *CSLE*s values. In the numerical simulation of Figure 3., only two stable *CSLE* solution can be found, however, it is easy to see, that exists a *CSLE* solution at *CSLE/D* = 0.302, which repels the *SLE* series. This behaviour shows, that two stable and one unstable *CSLE* coexist, corresponds to saddle-node bifurcation, which represents bistable parameter zone of a [19].

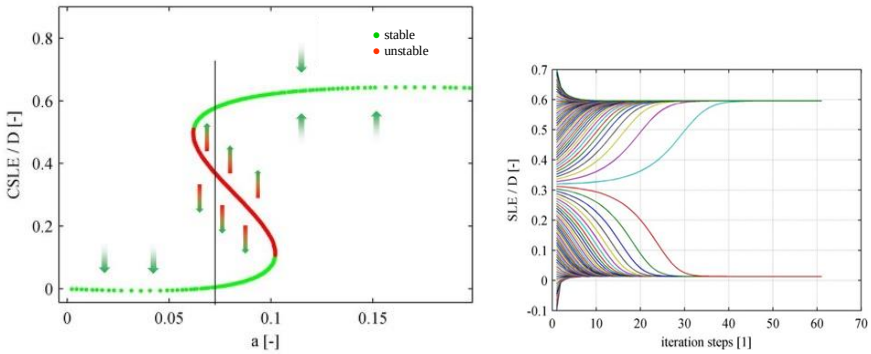

Figure 3. Multiple solutions of *CSLE*
a) *CSLE* calculated by MDBM
b) Numeric iteration along the black line at $a_0 = 0.07$
Parameters: $\Omega = 2250$ rad/s; $a_0 = 0.07$ -;$w = 4$ mm; $z = 1$; $f_z = 0.1$ mm

Both solution methods have their advantages and drawbacks. For instance, multiple steady state solution – in case of saddle-node or (fold) bifurcation – cannot be established and visualized properly via numeric iteration. On the other hand, an advantage of the iteration method is spectacular characteristic of periodic solutions and chaotic cascade can be detected and visualised, shown later in subsection Chaotic behaviour. With the help of MDBM, multiple and unstable solutions of Eq. (4) can also be obtained, but it does not provide information about the stability of the resultant *CSLE* values. However, stability properties can be determined with further computation steps, as it presented in the following section.

3. STABILITY ANALYSIS

The stability of the system depends on the derivative of the mapping equation. The solution is stable if the following equation is satisfied [20]:

$$-1 < \frac{\partial f_{SLE}}{\partial a_e}(CSLE) < 1. \qquad (8)$$

Derivative in Eq. (8) is produced by means of numeric derivation. Two possible instabilities can be observed in discrete mapping. Firs, when the derivative of the mapping equation is greater than 1. This case corresponds to the fold type bifurcation leading to bistable region. Second, when the derivative is smaller than -1. This situation corresponds to the period doubling or flip bifurcation. Thus, the resultant *CSLE* values can be coloured according its stability (in Figure 3.a, red and green dots represent the unstable and sable solutions, respectively).

Saddle-node (or fold type) bifurcation

The numerically determined *CSLE* in a proper region of the technological parameters (a, Ω) has a similar form as the well-known traditional cups catastrophe surface (see in Figure 4) [21]. The bifurcation diagram, the local stability of the steady states and certain sections of the catastrophe surface are given in Figure 4. Every theoretical observations – which are derived for the traditional catastrophe surface – are approximately valid for the *CSLE* as well. As shown in Figure 4.b, at a certain parameters ($a = 0.7922$, $\Omega = 4584$ rad/s), the dynamical system exhibits the classical supercritical pitchfork bifurcation. Light red regions shown the boundaries of the local stability of steady states at the rear and bottom side of Figure 4. The diagram at the bottom side (so-called cusp) features two regions: in the light red region at the bottom side there are three steady state solutions and beyond that region there is only one steady state solution.

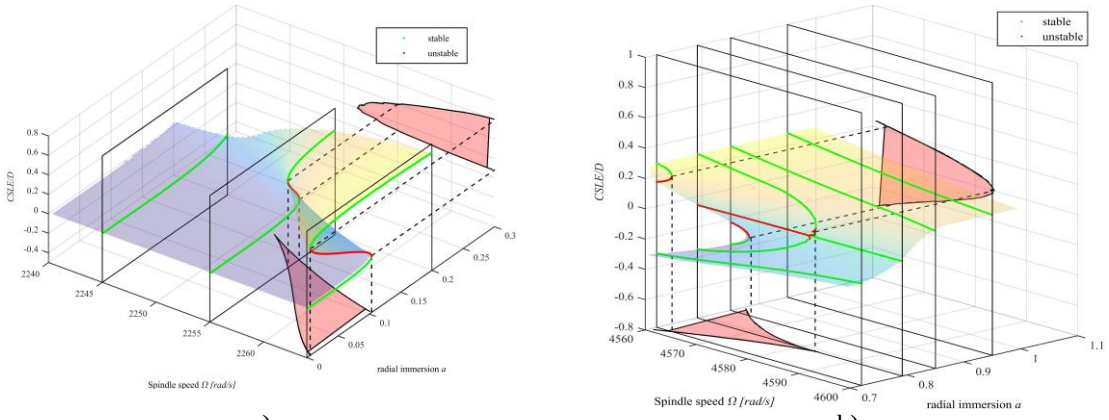

Figure 4. *CSLE* for different technological parameters (a, Ω); a) red area at the bottom side: region of three steady-states; Light red area at the rear side: unstable steady-state region;
Parameters: w = 4; mm; z = 1 ; f_z = 0.1 mm; Left: sections along spindle speed Ω;
b) sections along dimensionless radial immersion a; at section: a = 0.7916 – a classical supercritical pitchfork bifurcation is occurred

Period doubling (flip type) bifurcation

In a non-linear map, if flip-type bifurcation occurs, than it leads to period-2 solution. In our case, this is presented as an alternating *SLE* series in the numerical iteration. This behaviour can be detected by numerical simulation, only if this period-2 solution is stable. To discover all the stable and unstable period-2 solutions, two-step-mapping of Eq (4) must be considered in the MDBM method. The corresponding root finding problem of the two-step-mapping can be determined by a straightforward computation:

$$CSLE - f_{SLE}\left(a_0 + \frac{1}{D} f_{SLE}\left(a_0 + \frac{CSLE}{D}\right)\right) = 0 \qquad (9)$$

Note, that the results of Eq (9) will provide the periodic-2 solution together with the period-1 solution. The stability of this period-2 solution can be analysed in the same way as represented in Section 3. If a second flip-bifurcation is detected on a period-2 branch, then period-4 branch will occur, and the similar procedure have to be applied with four-step-mapping. For any further flip bifurcation, these steps have to be repeated.
The workflow of these process are summarised as the follows:

1. *Single* solution, derived based on one-step-mapping is established.
2. If the derivative of the map is smaller than -1, then flip type instability is occurred. So this *single* solution becomes unstable and creates a period-2 solution, represented by a pair of points in the bifurcation charts.
3. To obtain this doubled period-2 solution, two-step-mapping of the previous map have to be analysed.
4. If the derivative of this map is smaller than -1, then another flip bifurcation is occurred. And the iteration must be continued at point 3.
5. If the derivative of this map is not smaller than -1, then no more iteration is required.

Following this workflow, period-8 solution of *CSLE* could be found. In this figure, a fold bifurcation is also presented, so there can be cases, when flip bifurcation is occurred along one of the stable solution in a bistable zone.

At certain cutting parameters, there is a limit to this process, whereby cycles of period-2^n become unstable and bifurcate into stable cycles of period-2^{n+1}, creating a infinite many period doubling bifurcation cascade, which finally leads to chaos, in which there exist an infinite long of solution.

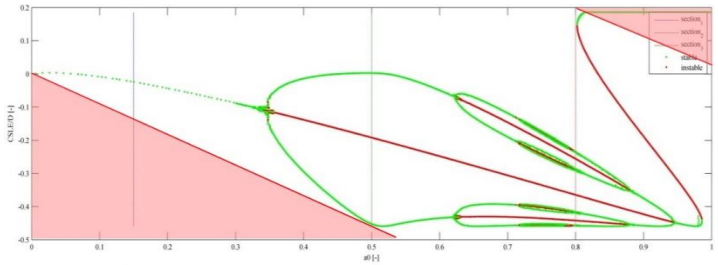

Figure 5. Period doubling bifurcations of the steady-state solution; green dots: stable solution, red dots, unstable solution, red area: physically invalid range
Parameters: Ω = 4551 rad/s; w = 3.5 mm; z = 1 ; f_z = 0.1 mm

Chaotic behaviour

In [22], the authors proved, that the periodic-n solutions are arranged in series as n = {2^0, 2^1, 2^2, …, 2^∞, 3^1, 3^2, …, 3^∞,5^1,…,}. If the period-3 exists, it means that period-2^∞ solutions necessarily also exist. Theoretically, the period-2^∞ solution repeats after an infinite long time (it is not a real periodic solutions), in other words, chaotic behaviour is occurred. In Figure 6. the bifurcation diagram is presented based on numerical iteration, it is clearly seen, that period-3 solution exists at $a \in [0.485, 0.493]$ and chaotic parameter windows are also occurred. The iteration of a chaotic series of *SLE*s at $a_0 = 0.52$ is presented in Figure 6.b.

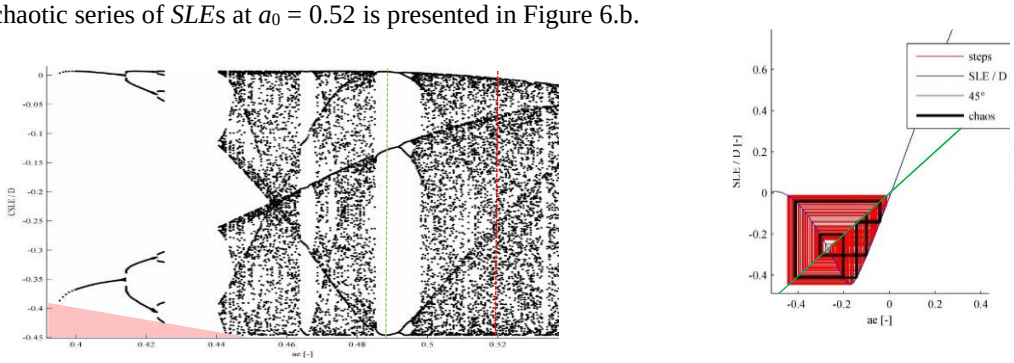

a) b)

Figure 6. a) Bifurcation diagram based on numeric iteration; Red area: physically invalid range; Green dashed line ($a_0 = 0.49$) denotes period-3 solution; Red dashed line ($a_0 = 0.52$) denotes chaotic solution; b) Mapping of *SLE* series in case of chaotic behaviour;
Parameters: Ω = 4551 rad/s; w = 7 mm; z = 1 ; f_z = 0.1 mm

4. *CSLE* MAP IN THE FUNCTION OF THE TECHNOLOGICAL PARAMETER SPACE

In this section, the *CSLE* is calculated in a large spindle speed range. The period doubling type and the saddle-node type instabilities are marked with red and blue colours, respectively, as shown in Figure 7. It can be seen that there are large *CSLE* if the spindle speed Ω close to a resonant one (see the black dashed vertical lines); in addition, period doubling or saddle-node bifurcation can be arisen at these region. Note, that some parameter domains, the calculated *CSLE* are constant along the radial immersion a due to the mathematical extension of f_{SLE} (see in subsection Range of validity).

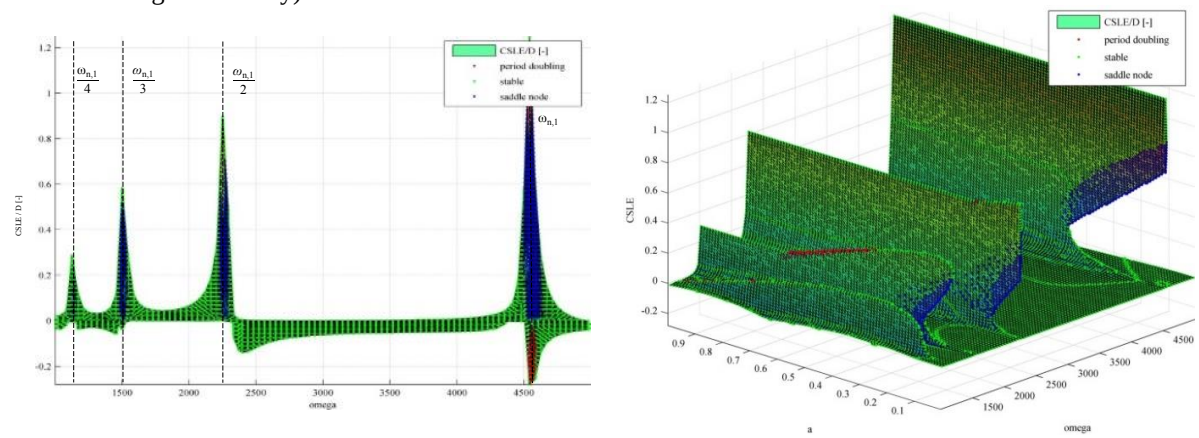

Figure 7. *CSLE* in the function of different technological parameters (a, Ω); Flip-type instability regions are indicated with red colour; Fold-type instability regions are indicated with blue colour;
Parameters: w = 7 mm; z = 1 ; f_z = 0.1 mm

The large stationary *CSLE* values would lead unacceptable shape error, but it can be compensated with a tool path offset. In case of bistable parameter range, it hard to predict which *CSLE* will evolved, thus, the tool path offset cannot determined in advance. The same situation occur, if non-stationary *CSLE* is formed (period-2, period-4, …, chaotic behaviour). The range of the technological parameters, where these instability problems occurs, should be avoid during roughing processes.

Bifurcation boundaries and stability chart

The boundary of these parameter range are defined by bifurcation points, where the derivative of the map is 1 or -1. The stability boundaries of the flip and fold bifurcations are presented separately together with the traditional stability chart [4] in the plane of the spindle speed Ω and dimensionless radial immersion a Figure 8. In our case, we applied the semi-discretization method to determine the stability chart [5]. Figure 8. shows that in the

favourable parameter domain between the stability lobes – the stability pockets – the stability problem of *CSLE* can be evolved.

The flip and fold bifurcations are correspond to series of the *SLE*s in roughing process, which based on the forced vibration only. This solution is linearly proportional to the axial immersion and the feed rate. Due to the fact that the traditional stability chart is independent to the feed rate, we can improve the domain of the *CSLE*-stable region, by decreasing the feed rate only.

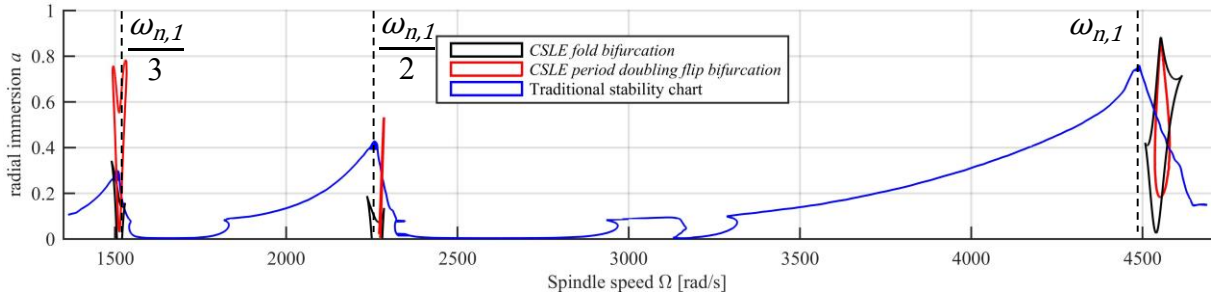

Figure 8. Stability charts, flip and fold bifurcations
Parameters: w = 1.5 mm; z = 1 ; f_z = 0.4 mm

5. CONCLUDING REMARKS

In the present study, we show a new type of stability problem, which can occur during roughing process. This *CSLE*-stability problem leads to an unpredictable final Surface Location Error, which can affect the finishing operation substantially. With the proposed methods, the traditional stability chart can be improved, from which chatter-free and *CSLE* stable technological parameters can selected.

In the future work, we will perform measurements to validate the theoretical results.

Acknowledgement

This paper was supported by the Hungarian Scientific Research Fund - OTKA PD-112983 and the Janos Bolyai Research Scholarship of the Hungarian Academy of Sciences.

REFERENCES

[1] S. A. TOBIAS, Machine tool vibration, *Blackie and Son, Ltd.*, London, 1965.
[2] J. TLUSTY, L. Spacek, Self-excited vibrations on machine tools, *Nakl. CSAV*, Prague. in Czech, 1954.
[3] G. STÉPÁN, Retarded Dynamical Systems, *Longman, Harlow*, 1989.
[4] B.P. MANN, K.A. YOUNG, T.L. SCHMITZ, D.N. DILEY, Simultaneous Stability and Surface Location Error Predictions in Milling. *Journal of Manufacturing Science and Engineering*, 127: 446–453. 2005.
[5] Y. ALTINTAS, E. BUDAK, Analytical prediction of stability lobes in milling. *Annals of the CIRP* 44/1:357–362. 1995.
[6] T. INSPERGER, G. STÉPÁN, Semi-Discretization for Time-Delay Systems, 1 ed. *Applied Mathematical Sciences. Springer*. 2011.
[7] D. BACHRATHY, G. STÉPÁN, Improved Prediction of Stability Lobes with Extended Multi Frequency Solution. *CIRP Annals – Manufacturing Technology* 62(1):411–414. 2013.
[8] T.L. SCHMITZ, B.P. MANN, Closed-form solutions for surface location error in milling, *International Journal of Machine Tools & Manufacture*, 46 (2006) 1369–1377, 2006.
[9] W. A. KLINE, R. E. DEVOR, I. A. SHAREEF, Prediction of surface accuracy in end milling, *ASME Journal of Engineering for Industry*, 104: 272–278. 1982.
[10] A. KISS, Cumulative surface location error for cutting processes, *MSc thesis, BME, Department of Applied Mechanics*, 2014.
[11] A. KISS, D. BACHRATHY, Experimental Validation of Cumulative Surface Location Error for Turning Processes, *14th Youth Symposium on Experimental Solid Mechanics*, Traunkirchen Monastery, Austria, 2015.
[12] D. BACHRATHY, T. INSPERGER, G. STÉPÁN, Surface properties of the machined workpiece for helical mills, *Machining Science and Technology*, 13(2), pp. 227–245., 2009.
[13] O. KIENZLE, Spezifische Schnittkrßafte bei der Metallbearbeitung, *Werkstattstechnik und Maschinenbau* 47, 224–225. 1957.
[14] J. TLUSTY, M. POLÁCEK, The stability of machine-tool against self-excited vibration in machining. *In Proceedings of the International Research in Production Engineering, American Society of Mechanical Engineers (ASME)*, Pittsburgh, PA, p. 465., 1963.
[15] D. BACHRATHY G. STÉPÁN, Efficient experimental detection of milling stability boundary and the optimal axial immersion for helical mills. *In Proceedings of International Multi-Conference on Engineering and Technological Innovation (IMETI 2008).* Orlando, Florida, USA (1): 7–11, ISBN 978-1-934272-46-6., 2008.
[16] G. PEIGNÉ, H. PARIS, D. BRISSAUD, Surface Shape prediction in high speed milling, *International Journal of Machine Tool & Manufacture*, Vol.44, No. 4, pp.1567-1576., 2004.
[17] J. GRADIŠEK, M. KALVERAM,T. INSPERGER, K. WEINERT,G. STÉPÁN, E. GOVEKAR, I. GRABEC, Stability prediction for milling. *International Journal of Machine Tools and Manufacture*, 45(7-8), pp. 769–781. 2005.
[18] D. BACHRATHY G. STÉPÁN, Bisection method in higher dimensions and the efficiency number. *Periodica Polytechnica Mechanical Engineering*, 56:(2) pp. 81-86; DOI: 10.3311/pp.me.2012-2.01, 2012.
[19] Y. A. KUZNETSOV, Elements of Applied Bifurcation Theory, Second Edition, Applied Mathematical Science, Springer 1998.
[20] J. T. SANDEFUR, Discrete Dynamical Systems : Theory and Applications, 1990.
[21] T. POSTON, I. STEWART, Catastrophe Theory and Its Applications, London: Pitman, 1978.
[22] TIEN-YIEN LI; JAMES A. YORKE, Period Three Implies Chaos; *The American Mathematical Monthly*, Vol. 82, No. 10. pp. 985-992, 1975.